Torque Analysis of a Radial Flux Air-Cored Permanent Magnet Machine with a Double-Sided Rotor and Non-Overlapping Windings

P.J. Randewijk and M.J. Kamper
Dept. of Electrical & Electronic Engineering, Stellenbosch University
Banhoek Road, Stellenbosch, 7600, South Africa
pjrandew@sun.ac.za

Abstract — The Radial Flux Air-Cored Permanent Magnet (RFAPM) machine is a permanent magnet (PM) machine that makes use of high energy-product rare-earth permanent magnets in order to utilise the advantages arising from using core-less – as well as non-overlapping stator windings. In this paper an analytical equation for the torque produced by a RFAPM machine with a Double-Sided Rotor and non-overlapping windings is presented by making use of subdomain analysis and the Lorentz method. The analytical results are compared with Finite Element Modelling (FEM) results.

I. INTRODUCTION

The RFAPM machine with a double-sided rotor and non-overlapping windings as shown in Fig. 1 was first presented by [1]. The advantage of the RFAPM machine is that the structural integrity of the cylindrical shaped rotor yokes are much higher than that of the disc shaped rotor yokes used in AFAPM machines [2], resulting in a 30% weight reduction over AFAPM machines for the same kVA rating due to thinner rotor yokes being used [3].

In this paper the modelling of the RFAPM machine is extended to include an analytical torque equation for the machine derived from an analytical field solution using the Lorentz method. The advantage of using the Lorentz method over the Maxwell stress tensor (MST) method for RFAPM (or AFAPM) machines, is that it only requires the radial flux density component caused by the PMs to be solved for the torque calculation. This is much more computational efficient than the MST method used in [4] for torque calculation or FEM in [5] for torque ripple optimisation as applied to AFAPM machines.

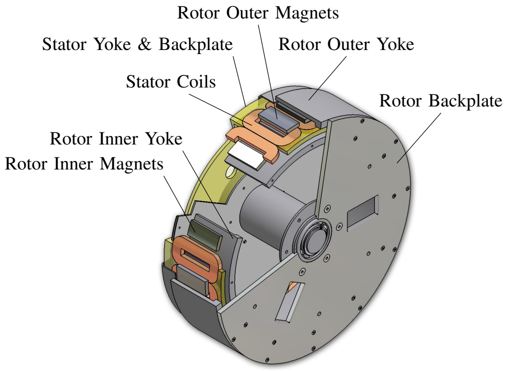

Fig. 1. A 3D view of a 24 pole RFAPM machine with concentrated coils.

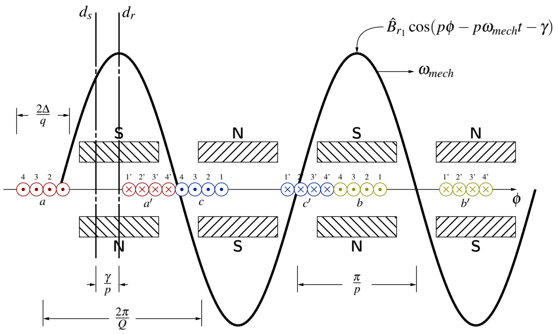

Fig. 2. Three-phase winding configuration for the RFAPM machine with a double-sided rotor and non-overlapping, double layer windings.

II. WINDING CONFIGURATION

In Fig. 2 the three-phase winding configuration for a Dual-Rotor RFAPM machine with non-overlapping double layer windings is shown.

This allows the current density distribution function for all three phases, assuming balanced sinusoidal currents, to be represented by the following Fourier series,

$$J_z = \begin{cases} -\frac{3qI_pN}{ar_nh\pi}\sum\limits_{m=1}^{\infty} k_{w,m}\sin\big(mq\phi + \omega t\big) & \text{for } m = 3k-1 \\ -\frac{3qI_pN}{ar_nh\pi}\sum\limits_{m=2}^{\infty} k_{w,m}\sin\big(mq\phi - \omega t\big) & \text{for } m = 3k-2 \end{cases} . \tag{1}$$

with $k \in \mathbb{N}_1$ for both cases and a the number of parallel circuits, q the number of coils per phase, N then number of turns per phase, I_p the peak current value per phase and $k_{w,m}$ the winding factor for the space harmonics.

III. SUBDOMAIN METHOD

The subdomain analytical analysis method [6] is used to solve the radial flux density in the stator region of the machine. The different regions are shown in Fig. 3 with the governing equation for each region given in Tabel I.

For the N48 NdFeB permanent magnets used, the relative recoil permeability are approximated to unity, [7], while the residual magnetisation is approximated to

$$\vec{\mathbf{M}}_0 \approx \frac{r_{cm}}{r}\cdot\frac{\vec{\mathbf{B}}_{rem}}{\mu_0} , \tag{2}$$

to simplify the analytical solution of the magnetic vector potential, [8].

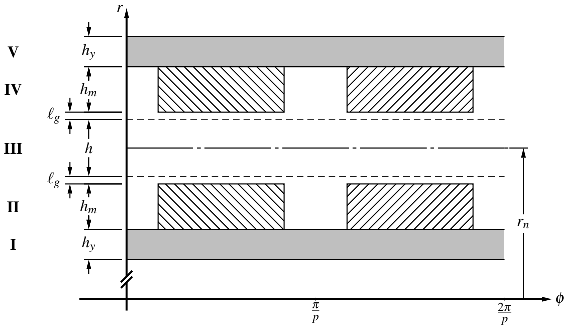

Fig. 3. A linear representation of the different regions.

Region	μ_r	Governing equation
I	μ_y	$\boldsymbol{\nabla}^2\vec{\mathbf{A}} = 0$
II	1	$\boldsymbol{\nabla}^2\vec{\mathbf{A}} = -\mu_0\left(\boldsymbol{\nabla}\times\vec{\mathbf{M}}_0\right)$
III	1	$\boldsymbol{\nabla}^2\vec{\mathbf{A}} = 0$
IV	1	$\boldsymbol{\nabla}^2\vec{\mathbf{A}} = -\mu_0\left(\boldsymbol{\nabla}\times\vec{\mathbf{M}}_0\right)$
V	μ_y	$\boldsymbol{\nabla}^2\vec{\mathbf{A}} = 0$

TABLE I
THE GOVERNING EQUATIONS FOR THE DIFFERENT REGIONS.

The solution of the radial flux density in the stator region are given by the following

$$B_{r|PM}(r,\phi) = -\frac{1}{r}\cdot\sum_{m=1,3,5,\ldots}^{\infty} mp(C^{III}_{m|PM} r^{mp} + D^{III}_{m|PM} r^{-mp})\sin mp\phi \tag{3}$$

with $C^{III}_{m|PM}$ and $D^{III}_{m|PM}$ the coefficients in the stator region, region III, solved from the boundary condition matrix up till the 27th harmonic, i.e. m=27.

Due to the "thinner" rotor yokes being used by the RFAPM machine, saturation of the rotor yokes were observed in the FEM analysis. The analytically calculated radial flux density was however only 3% higher compared to the FEM solution. This will subsequently also result in a 3% higher analytical calculated torque compared to the FEM solution.

IV. TORQUE CALCULATION

The Lorentz method for the mechanical torque, T_m,[1] is given by the following equation

$$T_m = \ell\int_{r_n-\frac{h}{2}}^{r_n+\frac{h}{2}}\int_0^{2\pi} r^2 J_z B_r\, d\phi\, dr\ , \tag{4}$$

with ℓ the active stack lengh. Solving this equation will yield the following solution

$$T_m = \begin{cases} -\frac{3q\ell N I_p}{a r_n h}\displaystyle\sum_{m=1,3,5,\ldots}^{\infty} k_{w,m} R_m S_{m,+} & \text{for } \ m = 3k-2 \\ -\frac{3q\ell N I_p}{a r_n h}\displaystyle\sum_{m=1,3,5,\ldots}^{\infty} k_{w,m} R_m S_{m,-} & \text{for } \ m = 3k-1 \end{cases} \tag{5}$$

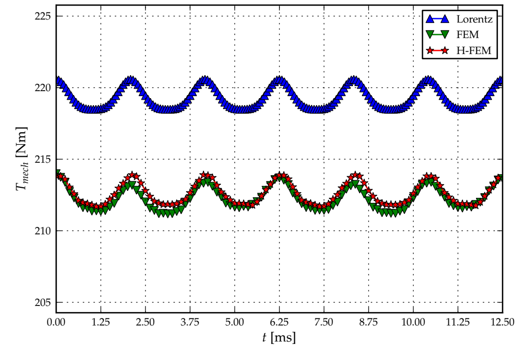

Fig. 4. The analytically calculated torque ripple for the RFAPM machine compared to a FEM and Hybrid-FEM solution.

with $k \in \mathbb{N}_1$ and

$$R_m = \int_{r_n-\frac{h}{2}}^{r_n+\frac{h}{2}} r^2 B_r\, dr \tag{6}$$

$$S_{m,+} = \cos(p\omega_m t)\cos(pm\omega_m t) + \sin(p\omega_m t)\sin(pm\omega_m t) \tag{7}$$

$$S_{m,-} = \cos(p\omega_m t)\cos(pm\omega_m t) - \sin(p\omega_m t)\sin(pm\omega_m t) \tag{8}$$

and displayed in Fig. 4 together with a FEM and a Hybrid-FEM solution.

V. CONCLUSIONS

The Lorentz method for the calculation of the torque compares well with that done using FEM. It is also very computational efficient compared to the MST method. For the conference paper measurements will also be included taken from a 6.75 kW prototype that was built.

VI. REFERENCES

[1] P. J. Randewijk, M. J. Kamper, and R. J. Wang, "Analysis and performance evaluation of radial flux air-cored permanent magnet machines with concentrated coils," in *Power Electronics and Drive Systems, 2007. PEDS '07. 7th International Conference on*, 2007, pp. 189–195.

[2] R.-J. Wang, M. J. Kamper, K. Van der Westhuizen, and J. F. Gieras, "Optimal design of a coreless stator axial flux permanent-magnet generator," *Magnetics, IEEE Transactions on*, vol. 41, no. 1, pp. 55–64, 2005.

[3] J. A. Stegmann and M. J. Kamper, "Design aspects of medium power double rotor radial flux air-cored pm wind generators," in *Energy Conversion Congress and Exposition, 2009. ECCE 2009. IEEE*, Sept. 2009, pp. 3634–3640.

[4] P. Virtic, P. Pisek, M. Hadziselimovic, T. Marcic, and B. Stumberger, "Torque analysis of an axial flux permanent magnet synchronous machine by using analytical magnetic field calculation," *Magnetics, IEEE Transactions on*, vol. 45, no. 3, pp. 1036 –1039, Mar. 2009.

[5] C.-C. Hwang, P.-L. Li, F. Chuang, C.-T. Liu, and K.-H. Huang, "Optimization for reduction of torque ripple in an axial flux permanent magnet machine," *Magnetics, IEEE Transactions on*, vol. 45, no. 3, pp. 1760 –1763, Mar. 2009.

[6] Z. Zhu, L. Wu, and Z. Xia, "An accurate subdomain model for magnetic field computation in slotted surface-mounted permanent-magnet machines," *Magnetics, IEEE Transactions on*, vol. 46, no. 4, pp. 1100 –1115, Apr. 2010.

[7] P. Kumar and P. Bauer, "Improved analytical model of a permanent-magnet brushless dc motor," *Magnetics, IEEE Transactions on*, vol. 44, no. 10, pp. 2299–2309, Oct. 2008.

[8] S. R. Holm, H. Polinder, and J. A. Ferreira, "Analytical modeling of a permanent-magnet synchronous machine in a flywheel," *Magnetics, IEEE Transactions on*, vol. 43, no. 5, pp. 1955–1967, May 2007.

---

[1] The subscript "m" in T_m and ω_m refers to the mechanical torque and mechanical speed of the machine and not the space harmonic number.